ELSEVIER

Chemical Engineering Journal 81 (2001) 203–212

Chemical Engineering Journal

www.elsevier.com/locate/cej

Enhancement of gas–liquid mass transfer by small reactive particles at realistically high mass transfer coefficients: absorption of sulfur dioxide into aqueous slurries of $Ca(OH)_2$ and $Mg(OH)_2$ particles

Manoj V. Dagaonkar [a], Antonie A.C.M. Beenackers [a,*], Vishwas G. Pangarkar [b]

[a] *Department of Chemical Engineering, University of Groningen, Nijenborgh 4, 9747 AG Groningen, The Netherlands*
[b] *Department of Chemical Engineering, University of Mumbai, Matunga, Mumbai 400019, India*

Received 1 December 1999; received in revised form 31 May 2000; accepted 12 June 2000

Abstract

Chemical absorption of pure SO_2 into aqueous slurries of fine and reactive $Ca(OH)_2$ and $Mg(OH)_2$ was studied in a stirred vessel at 298 K at realistically high mass transfer coefficients. The absorption process was theoretically analyzed using two different models. For the SO_2–$Ca(OH)_2$ system, a single reaction plane model was used to estimate the theoretical enhancement factor and for the SO_2–$Mg(OH)_2$ system, a two-reaction plane model incorporating the solids dissolution promoted by the reactions with the absorbed SO_2 in the liquid film was employed. For the later system, the theoretical results could be more accurately predicted by a correct approach to estimate the enhancement caused due to suspended solids and the overall enhancement factor. The extra enhancement observed for the SO_2–$Mg(OH)_2$ system could be explained from the reaction between SO_2 and the dissolved $[SO_3]^{2-}$. © 2001 Elsevier Science B.V. All rights reserved.

Keywords: Reactive solids; Enhancement; Solid dissolution; Calcium hydroxide; Magnesium hydroxide; Sulfur dioxide

1. Introduction

Slurry reactors have a widespread application in chemical and bio-chemical industries. The problem of gas absorption with reaction in a slurry containing fine particles has become important in the development of processes for the removal of acidic pollutants. At present, most wet scrubbing processes for the removal of SO_2 are by lime and limestone slurry solutions. Also $Mg(OH)_2$ as suspended solids may yield a high scrubbing capacity as a result of the presence of the more soluble reaction product magnesium sulfite, relative to the corresponding calcium salt.

The present work focuses on the enhancement of the absorption rate of a gas into a slurry containing small reactive particles. The elementary processes involved in chemical absorption into the slurry are

1. diffusion of the solute gas in the film,
2. chemical reaction,
3. dissolution of solid.

Applying the so called film theory for mass transfer, the chemical absorption and the solids dissolution are transfer processes either in series or in parallel, depending upon whether the suspended particles size is significantly smaller or larger than the thickness of the liquid film (film model, film thickness $= D/k_L$). The solids dissolution in the liquid film enhances the absorption rate and further the rate of solute dissolution is enhanced by the reaction between the dissolved gas and the dissolved solid in the liquid film when the particle size is significantly smaller than the film thickness. As a result, the solid dissolution rate as well as the chemical reaction rate affect the rate of gas absorption.

2. Previous work

Table 1 summarizes the literature data reported for the absorption of SO_2 into aqueous slurries of calcium and magnesium hydroxides and the corresponding enhancement factors observed. Here, E_0 is the enhancement factor in the absence of suspended particles and E is the enhancement factor under similar conditions but with suspended particles present.

This problem has been discussed on the basis of the film model by Ramachandran and Sharma [1] considering the effect of solids dissolution in the liquid film both, to be important and not important depending on the conditions.

* Corresponding author. Tel.: +31-50-3634486; fax: +31-50-3634479.
E-mail address: A.A.C.M.Beenackers@chem.rug.nl (A.A.C.M. Beenackers).

1385-8947/01/$ – see front matter © 2001 Elsevier Science B.V. All rights reserved.
PII: S1385-8947(00)00214-X

Nomenclature

A^*	concentration of A at the gas–liquid interface (mol/m^3)
A_p	$6w/\rho\ d_p$, surface area of solid particle (m^2/m^3-dispersion)
a	gas–liquid interfacial area (m^2/m^3 liquid)
C	concentration in the liquid phase (mol/m^3)
D	diffusivity in the liquid phase (m^2/s)
d_p	arithmatic mean particle diameter (m) as defined by $d_i^2 = (\sum n_i d_i^2)/(\sum n_i)$
E	enhancement factor
He	Henry's constant (Pa m^3/mole)
J	mass transfer rate (mol/m^2 s)
k_L	liquid side mass transfer coefficient (m/s)
k_s	solid side mass transfer coefficient (m/s)
m	$\sqrt{k_s A_p / D_B}$
N	$k_s A_p z_L^2 / D_B$ solid dissolution parameter
N_A	moles of A absorbed
n	stirring speed (s^{-1})
p	partial pressure of the solute gas (Pa)
q_A	C_{Ai}/C_{Bs}
R	gas constant (J/mole K)
r_A	D_A/D_B
T	Temperature (K)
t	time (s)
V_L	liquid volume (m^3)
V_G	gas volume (m^3)
w	amount of solids (mol/m^3 slurry)
x_1	dimensionless position of the first reaction plane
Y	dimensionless concentration in liquid phase relative to that at gas–liquid interface or at solid surface
z_1	position of the first reaction plane as shown in Fig. 5b (m)
z_L	thickness of liquid film as shown in Fig. 5b (m)

Greek letters

ρ	density of solid particle (kg/m^3)
ν	overall reaction stoichiometry
λ	reaction plane for SO_2–$Ca(OH)_2$ system (m)
δ	film thickness for SO_2–$Ca(OH)_2$ system (m)

Subscripts

A	component A (SO_2)
B	component B $[OH]^-$
F	component F $[HSO_3]^-$
E	component E $[SO_3]^{2-}$
i	value at gas–liquid interface
0	value in the absence of suspended particles ($N = 0$)
s	at the surface of the solid particle

Superscripts

0	value at time $t = 0$
∞	value at time $t = \infty$

Later, Uchida et al. [2] modified the model proposed by Ramachandran and Sharma and pointed out that the rate of solids dissolution is enhanced by the reaction between the absorbed gas and the dissolved solid in the liquid film. Sada et al. [3–6] formulated the process of gas absorption in the slurry on the basis of the film model incorporating instantaneous reactions between the absorbed gas and the dissolved solid in the liquid of the film. Their model assumes that solids dissolution in the film for mass transfer is one of the elementary steps. This is the case when the average size of the suspended particles is considerably smaller than the thickness of the film. The reaction was interpreted both, by a single reaction plane model [3] and a two-reaction plane model [4], respectively. The validity of the proposed model was checked by single and simultaneous absorption of CO_2, or NO_2 and/ or SO_2 into aqueous slurries of $Ca(OH)_2$ [4,7,8] and by the absorption of SO_2 into aqueous slurries of $Mg(OH)_2$ using a stirred-tank absorber with a flat gas–liquid interface. However, the experimental results for high SO_2 concentrations could not be interpreted by the proposed models [6], possibly because these did not incorporate the fact that the solids dissolution in the liquid film can be enhanced by the chemical reactions.

Sada et al. [9] developed a two-reaction plane model incorporating the solids dissolution enhanced by the reactions in the liquid film. The theoretical enhancement factors compared well with the experimental data.

The particles of $Ca(OH)_2$ and $Mg(OH)_2$ being reactive, help to increase the rate of absorption of SO_2 in the slurry. Previous authors have measured the enhancement factor at a speed range of 1–4 s^{-1} which gives a very low mass transfer coefficient ($2–4\times10^{-5}$ m/s) which is much lower than applied in industrial practice. The purpose of the present work is to present the absorption data for the removal of SO_2 by micro sized reactive particles of calcium and magnesium hydroxide at stirring speeds in the range of 3–15 s^{-1} ($Re > 10^5$) and to check whether the experimentally observed enhancement factors can be described by a suitable model.

3. Experimental investigations

The experiments were carried out in a thermostatted reactor of glass and stainless steel as shown in Fig. 1. A six bladed turbine stirrer was located centrally in the liquid at a height above the reactor bottom equal to half the reactor diameter. Four symmetrically mounted glass baffles increased the effectiveness of stirring and prevented the formation of a vortex. The pressure and temperature transducers together with valves 1 and 2 were connected to an Olivetti M240 computer, thus enabling automatic data collection

Table 1
Literature review for the absorption of SO_2 in hydroxide slurries

S. no.	Gas–slurry system	Gas concentration	Solids (wt.%)	Enhancement factor
1	SO_2 in aqueous slurries of $Mg(OH)_2$ particles [10]	5%	0–20%	$E/E_0 = 1 - 2.3$
2	SO_2/CO_2 absorption in $Ca(OH)_2$ slurry [3]	5%	0–30%	1–4
3	SO_2/CO_2 absorption in $Ca(OH)_2$ slurry [7]	2000–4800 Pa	0–20%	1–3
4	Absorption of lean SO_2 in aqueous solutions of Na_2SO_3 [5]	$SO_2 + N_2$ + watervapour	0–300 mol/m^3	1–15
5	Absorption of lean SO_2 and NO_2 into aqueous slurries of $Ca(OH)_2$ or $Mg(OH)_2$ [8]	800–10,000 ppm	0–15%	$E/E_0 = 1$–3
6	Absorption of SO_2 in aqueous slurries of $Mg(OH)_2/CaCO_3$ [14]	100–1000 ppm	2–10%	2–10
7	Absorption of SO_2 in $Mg(OH)_2/CaCO_3$ slurry [4]	100–2000 ppm	0–10%	1–5
8	Absorption of SO_2 in $Mg(OH)_2/CaCO_3$ slurry [16]	2000 ppm	0.5% $CaCO_3$ 3% $Mg(OH)_2$	1–10 1–40
9	Absorption of lean SO_2 into aqueous slurries of $CaCO_3$ and $Mg(OH)_2$ [9]	100–2000 ppm	1–5%	$E/E_0 = 1$–5
10	Absorption of SO_2 by calcium hydroxide solution in a wetted wall column: effect of magnesium hydroxide, magnesium carbonate and magnesium sulfite additives [17]	1000–5000 ppm	$Ca(OH)_2$: 0.0106 M $Mg(OH)_2$: 0.0001883 M	5–80
11	Chemical absorption of CO_2 and SO_2 into $Ca(OH)_2$ slurry [13]	Pure SO_2 diluted by N_2	0–20%	1–7
12	Absorption of CO_2 and SO_2 into aq. Conc. Slurries of $Ca(OH)_2$ [18]	10^5 Pa	2–40%	1–3
13	Absorption of SO_2 into aq. Double slurries containing limestone and $Mg(OH)_2$ [19]	1715 ppm	$CaCO_3$: 1–3% $Mg(OH)_2$: 0.25–1%	1–3
14	Absorption of SO_2 in $Ca(OH)_2/CaSO_3$ [20]	0–1000 ppm	$CaSO_3$: 1–7% $NaHSO_3 + Na_2SO_3$ 2 M	5–20 1.2–2.2
15	Absorption of SO_2 in $Mg(OH)/CaCO_3$ [15]	0–1000 ppm	$Mg(OH)_2$: 0–5%	5–10

and programmed reactor operation. The reactor dimensions are given in Table 2.

After filling the reactor with the desired slurry, the liquid was degassed by closing valve 1 and opening valve 2. Once the slurry was equilibrated under the vapour pressure of water, N_2O was fed to the reactor upto a fixed pressure (0.8×10^5 Pa). Then, the stirrer was started and the decrease of pressure due to the physical absorption of N_2O was recorded over time. These data were used to estimate the solubility of the gas and the liquid side mass transfer coefficient. The operating conditions of the reactor are listed in Table 3.

Table 2
Reactor dimensions

Reactor diameter	0.105 m
Reactor volume	1.777×10^{-3} m^3
Gas–liquid contact area	8.37×10^{-3} m^2
Liquid impeller type	Six bladed turbine, 0.04 m diameter
Gas impeller type	Six bladed turbine, 0.06 m diameter with enlarged six blades

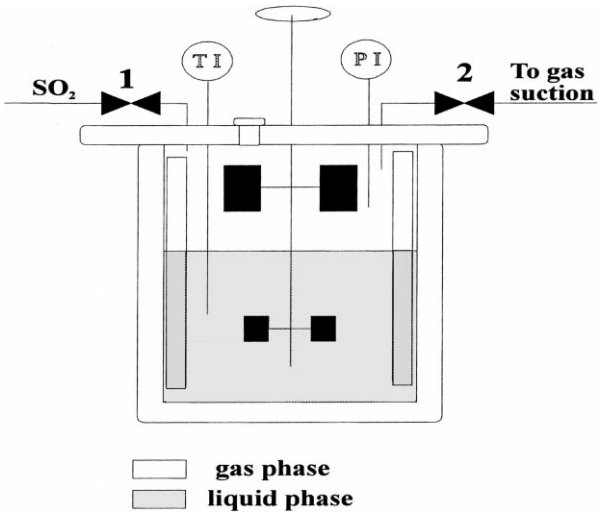

Fig. 1. Stirred cell reactor (1, 2: computer activated valves, 3: thermostates stainless steel top, 4: thermostated glass reactor wall, 5: Medimix magnetic coupling, 6: gas stirrer, 7: liquid stirrer).

After the physical absorption experiments, the chemical absorption of pure SO_2 into aqueous slurries of $Ca(OH)_2$ and $Mg(OH)_2$ was carried out. All the experiments carried out were batchwise, both, with respect to gas phase and the slurry solution. The volume of the slurry loaded in the reactor was always kept at 10^{-3} m^3 and the slurry concentration

Table 3
Experimental conditions

Temperature	25°C
Initial pressure	0.8×10^5 Pa
Liquid volume	1×10^{-3} m^3
Gas	N_2O, purity >99.5% SO_2, purity >99.5
Stirrer speed	3–13 s^{-1}

Table 4
Data used in the experimental calculations

d_p $Ca(OH)_2 = 4.5\,\mu m$ (determined with Coulter Counter)
d_p $Mg(OH)_2 = 21.4\,\mu m$ (determined with Coulter Counter)
$D_{SO_2-water} = 1.49 \times 10^{-9}\,m^2/s$ [3]
$D_{N_2O-water} = 1.78 \times 10^{-9}\,m^2/s$ [3]
$D_{CO_2-water} = 1.95 \times 10^{-9}\,m^2/s$ [3]
C_{Bs} of $Ca(OH)_2$ in water $= 23\,mol/m^3$ [8]
C_{Bs} of $Mg(OH)_2$ in water $= 0.46\,mol/m^3$ [8]
$T = 298\,K$
He for SO_2–water sytem $= 73.01\,Pa\,m^3/mol$ [19]

was varied from 0 to 20 wt.%. Table 4 gives the data used in the experimental calculations. The reactive particles of $Ca(OH)_2$ and $Mg(OH)_2$ of arithmatic mean size 4.5 and 21.2 μm were used for the experimentation. Table 5 gives the size distribution of these particles.

The interfacial area at higher speeds ($N > 6.5\,s^{-1}$) where the gas–liquid interface is no longer flat, was obtained from the absorption rate of carbon dioxide into a $3000\,mol/m^3$ NaCl solution containing 100–1000 mol/m^3 NaOH. CO_2 pressure was kept at 2500 Pa. Due to the presence of NaOH, the absorption of CO_2 is enhanced relative to the physical absorption. The interfacial area then can be calculated by the standard procedure reported by Mehta and Sharma [10]. The interfacial area was found to remain unaffected in the speed range of 3–15 s^{-1}. The information regarding the effect of solids on the interfacial area for the stirred cell is so scattered that no reliable correlation can be presented. Literature has been reported only for bubble columns and stirred cells with gas spargers. Increase in the solid content results in increase in the percentage of gas–liquid surface coverage suggesting an increase in the interfacial area [11]. In our case as the gas phase is above the G/L interface, this effect of the presence of solids on the interfacial area could be neglected due to the absence of bubbles.

4. Estimation of gas solubilities and mass transfer coefficients

The solubility of a gas A in a liquid defined as the Henry coefficient, is expressed by

$$He = \left(\frac{P_A}{C^i}\right)_{\text{at equilibrium}} \tag{1}$$

Table 5
Size distribution of the hydroxide particles

% Particles	Particle size (μm)	
	$Ca(OH)_2$	$Mg(OH)_2$
10	6.09	29.16
25	4.71	24.44
50	3.52	18.38
75	3.34	16.57
90	3.24	15.65
Arithmatic mean size	4.35	21.20

In the absence of chemical reaction the concentration of the gas in the liquid follows directly from the total amount of gas absorbed. For an ideal gas

$$He = \frac{(p^\infty - p^{H_2O})}{(p^0 - p^\infty)}\frac{RTV_L}{V_G} \tag{2}$$

Volumetric mass transfer coefficients were obtained from the physical absorption rate of nitrous oxide with time. The value of $k_L a$ follows from

$$\left(\frac{k}{k+1}\right)\ln\left(\frac{p_A^0}{(k+1)p_A - kp_A^0}\right) = k_L a t \tag{3}$$

where

$$k = \left(\frac{V_G\,He}{V_L RT}\right) \tag{4}$$

The volumetric mass transfer coefficient of physical absorption of SO_2 in water then follows from [5]

$$(k_L a)_{SO_2} = (k_L a)_{N_2O}\left(\frac{D_{SO_2-water}}{D_{N_2O-water}}\right)^{2/3} \tag{5}$$

The rate of $SO_{2\,absoption}$ in the slurry follows from

$$J_A a = \frac{V_G}{V_L RT}\left(\frac{-dP_A}{dt}\right) = k_L E C_{Ai} \tag{6}$$

The experimental enhancement factor was calculated by taking the ratio of the initial rates in presence of the solids and in the absence of suspended solid particles i.e. the saturated solution of the hydroxide involved. If $E_A > 1$, the absorption is chemically enhanced whereas $E_A = 1$ represents a purely physical absorption of SO_2.

5. Theory of gas absorption

5.1. SO_2 absorption in $Ca(OH)_2$ slurry

$[SO_3]^{2-}$ produced by the reaction of SO_2 and $[OH]^-$ is gradually accumulated. $[OH]^-$ ions are fed by the dissolution of the solid particles in the liquid film. In the case of the SO_2–$Ca(OH)_2$ system the reaction between SO_2 and $[OH]^-$ is instantaneous and the product of the reaction $CaSO_3$ is insoluble in the medium [12]. The reaction scheme for this process of gas absorption can be represented as

$$SO_{2(g)} \rightarrow SO_{2(aq)} \tag{i}$$

$$Ca(OH)_{2(s)} \rightarrow [Ca]^{2+} + 2[OH]^- \tag{ii}$$

$$SO_{2(aq)} + 2[OH]^- \rightarrow [SO_3]^{2-} + H_2O \tag{iii}$$

As the rate of solid dissolution is enhanced by the instantaneous reaction of SO_2 and $Ca(OH)_2$, the model proposed by Uchida et al. [2] can be used to describe the absorption process. The rate of gas absorption is given by the expression

$$J_A = mD_A A^* \coth m\lambda + \frac{mD_B C_{Bs}}{z}\left(\coth m\lambda - \frac{1}{\sinh m\lambda}\right) \quad (7)$$

The parameter λ can be calculated by the equation

$$\frac{D_B C_{Bs}}{2}\left(\coth m\lambda + \coth m(\delta-\lambda) - \frac{1}{\sinh m\lambda}\right) - \frac{D_A A^*}{\sinh m\lambda} = 0 \quad (8)$$

when the solution contains no suspended solids, the expression becomes

$$J_0 = k_L A^*\left(1 + \frac{D_B B_s}{D_A A^*}\right) \quad (9)$$

5.2. SO_2 absorption in $Mg(OH)_2$ slurry

In the SO_2–$Mg(OH)_2$ slurry process, however, the product of the reaction $MgSO_3$ has a much higher solubility in water than that of $Mg(OH)_2$. The species $MgSO_3$ formed exists in a dissolved state. The dissolved SO_2 thus also reacts with $[SO_3]^{2-}$ and forms $[HSO_3]^-$ which in turn further enhances the rate of absorption. Thus, dissolved SO_2 is consumed by the reaction scheme of

$$SO_2 + 2[OH]^- = [SO_3]^{2-} + H_2O \quad (I)$$

$$SO_2 + [SO_3]^{2-} + H_2O = 2[HSO_3]^- \quad (II)$$

$$[HSO_3]^- + [OH]^- = [SO_3]^{2-} + H_2O \quad (III)$$

In the process of SO_2 absorption in $Mg(OH)_2$ slurry with no suspended particles, $[HSO_3]^-$ cannot coexist with $[OH]^-$, so that reaction (I) never takes place directly (see Fig. 2a). The above consideration shows that reactions (II) and (III) take place at two differently located planes in the two-reaction plane model. However, in the slurry process to be considered here, both dissolved SO_2 and the $[HSO_3]^-$ to be produced by reaction (II) can react with $[OH]^-$ which is fed by the dissolution of the solid particles in the liquid film. So in this case, dissolved SO_2 can be consumed by reactions (I) and (II) simultaneously. The concentration of $[SO_3]^{2-}$ in the bulk liquid increases as the absorption proceeds.

For a saturated solution of magnesium hydroxide, a plausible sketch of the concentration profile is given in Fig. 2(a). When the particles are suspended in the liquid film, the concentration profiles shift as shown in Fig. 2(b).

5.2.1. Reaction plane model

The mass balances for the relevant species in the regions I, II and II are as follows

Region I

$$D_A\frac{d^2C_A}{dz^2} - \frac{k_s}{2}\left(1 + \frac{2D_A C_A}{C_{Bs}D_B}\right)A_p C_{Bs} = 0 \quad (10)$$

$$D_F\frac{d^2C_F}{dz^2} - k_s\left(1 + \frac{D_F C_F}{C_{Bs}D_B}\right)A_p C_{Bs} = 0 \quad (11)$$

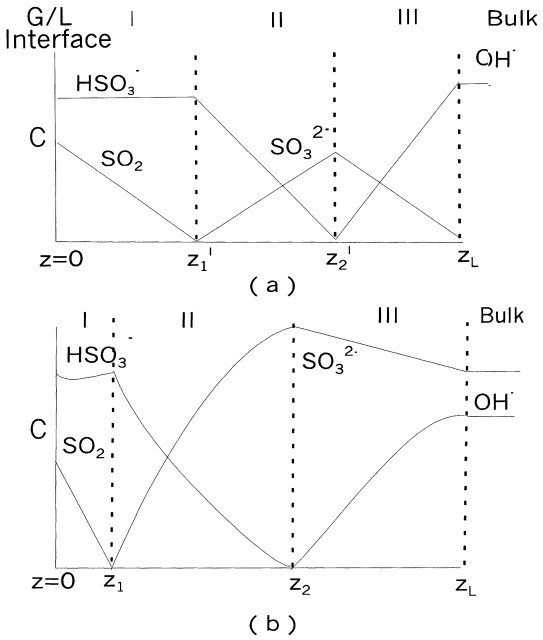

Fig. 2. Concentration profiles based on two-reaction plane model for the SO_2–magnesium hydroxide system. (a: no suspended solids, b: in presence of suspended solids).

Region II

$$D_F\frac{d^2C_F}{dz^2} - k_s\left(1 + \frac{D_F C_F}{C_{Bs}D_B}\right)A_p C_{Bs} = 0 \quad (12)$$

$$D_E\frac{d^2C_E}{dz^2} + k_s\left(1 + \frac{D_F C_F}{C_{Bs}D_B}\right)A_p C_{Bs} = 0 \quad (13)$$

Region III

$$D_B\frac{d^2C_B}{dz^2} + k_s A_p(C_{Bs} - C_B) = 0 \quad (14)$$

$$D_E\frac{d^2C_E}{dz^2} = 0 \quad (15)$$

The boundary conditions imposed are

$$\text{At } z = 0, \quad C_A = C_{Ai}, \ \frac{dC_F}{dz} = 0 \quad (16)$$

$$z = z_1, \quad C_A = C_E = 0, \ C_F = C_F^* \quad (17)$$

$$-D_A\left(\frac{dC_A}{dz}\right) = D_E\left(\frac{dC_E}{dz}\right) \quad (18)$$

$$\text{At } z = z_2, \quad C_B = C_F, \ C_E = C_E^* \quad (19)$$

$$D_B\left(\frac{dC_B}{dz}\right) = -D_F\left(\frac{dC_F}{dz}\right) \quad (20)$$

$$\text{At } z = z_L, \quad C_B = C_{Bs}, \quad C_E = C_{E0} \quad (21)$$

C_E^* and C_F^* represent the concentrations of E at z_2 and F at z_1, respectively (A = SO_2, B = $[OH]^-$, E = $[SO_3]^{2-}$, F = $[HSO_3]^-$).

The expression for the enhancement factor obtained by solving Eq. (10) with the given boundary conditions [9] is

$$E=\left[1+\frac{1}{2r_A q_A}\right]\frac{\sqrt{N}}{\tan\sqrt{N}x_1}-\left[\frac{1}{2r_A q_A}\right]\frac{\sqrt{N}}{\sinh\sqrt{N}x_1} \quad (22)$$

E_0 represents the enhancement factor for a clear solution saturated with the hydroxides and is defined by

$$E=\left[1+\frac{1}{2r_A q_A}\right] \quad (23)$$

6. Results and discussion

6.1. Effect of speed of agitation on k_L^0

Experimental results for the physical absorption of N_2O in calcium and magnesium hydroxide slurries are plotted in Fig. 3(a) and (b) as k_L^0 versus n with the slurry concentration as a parameter. The series of experimental points fall on a straight line with a slope of 0.8, irrespective of the slurry concentration. This is in close agreement with the previously reported results for such type of agitated absorption vessel [10]. The contribution of the gas side resistance was zero as pure SO_2 was used. The initial pressure was kept constant (800 mbar) for all the experiments.

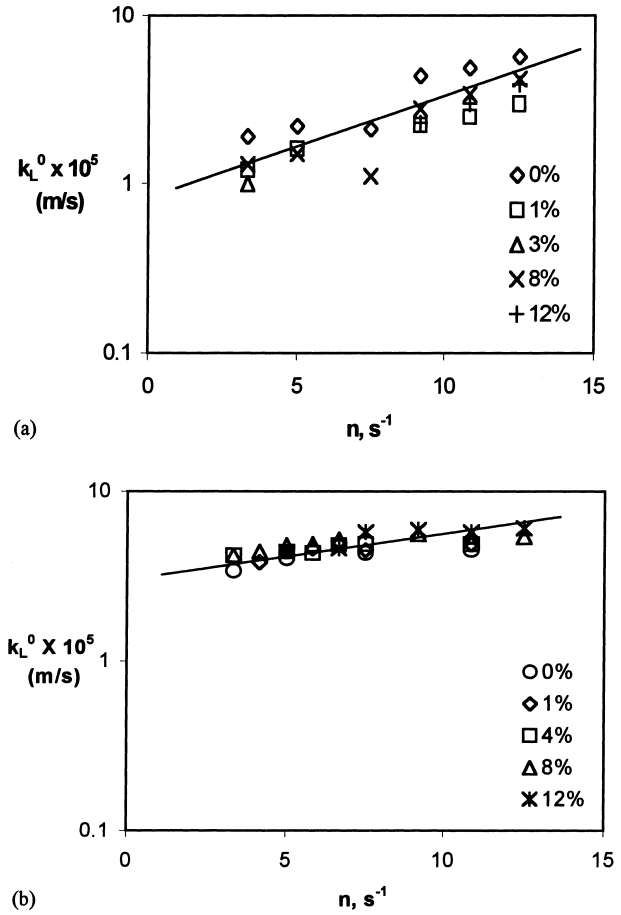

Fig. 3. Effect of stirrer speed of agitation on liquid side mass transfer coefficient at different solid loading (wt.%). (a: system: $N_2O/Ca(OH)_2$ slurry, b: system: $N_2O/Mg(OH)_2$ slurry, initial pressure $= 0.8 \times 10^5$ Pa, $T = 298$ K).

6.2. Effect of solid loading

To show the contribution of the presence of the solids to the absorption rate, the ratio of enhancement factor into slurry to that into saturated solution (E/E_0) is plotted against wt.% solids in Fig. 4(a) and (b). The ratio E/E_0 represents the degree of enhancement owing to the presence of solid particles in the slurry.

For the case of SO_2 absorption in $Ca(OH)_2$ slurry, the concentration of $[SO_3]^{2-}$ (in the bulk) to be produced by the reaction of SO_2 and $Ca(OH)_2$ is extremely low, because the solubility of $CaSO_3$ in water is about 25 times lower than that of $Ca(OH)_2$ [10]. Consequently, the reaction between dissolved SO_2 and $[SO_3]^{2-}$ can be neglected. The solid curves plotted in Fig. 4a (Lines 1, 2, 3, 4 and 5) are obtained from the theoretical values of the enhancement factor. These theoretical values are calculated using the model proposed by Uchida et al. [2], by using Eqs. (7)–(9). Table 6 shows the experimental values of the enhancement factor under the different experimental conditions.

In order to compare the experimental results with the theoretical predictions for the SO_2–$Mg(OH)_2$ system, it is necessary to know the values of the dimensionless parameters r, q and N. For the evaluation of r, the diffusivity of SO_2 in the slurry was assumed to be the same as that in pure water. Thus, the value of r is 1.22 for this system. The value of q was calculated from the ratio of concentration of SO_2 at the gas–liquid interface and the solubility of the hydroxide in water. The dimensionless distances into the liquid phase from the gas–liquid interface (x_1 and x_2) were calculated computationally by using the equations suggested by Sada et al. [8]. The position of the primary reaction plane was smaller than the average diameter of the suspended particles, typically z_1/d_p was in the range of 0.4–0.45.

The dimensionless parameter N is proportional to the solid concentration in the slurry solution (w). Fig. 4b gives the variation of E/E_0 with the solid loading for the absorption of SO_2 in $Mg(OH)_2$ slurry and its values are also indicated in Table 7. For the estimation of the parameter N, Sada et al. [9] compared their experimental results with the theoretical prediction according to model II [8,10]. However, as model II did not take into account the extra reaction between SO_2 and $[SO_3]^{2-}$ (reaction II), the values of experimental enhancement factors predicted by Sada et al. [9] did not match with the theoretical values predicted by Model II [8,10].

The enhancement observed in this system is considered to be attributed due to both the presence of solid particles (reactant of reaction I and III) in the liquid film and the extra reaction of SO_2 and $[SO_3]^{2-}$ (reaction II). The concentration of $[SO_3]^{2-}$ is allowed to be a function of time.

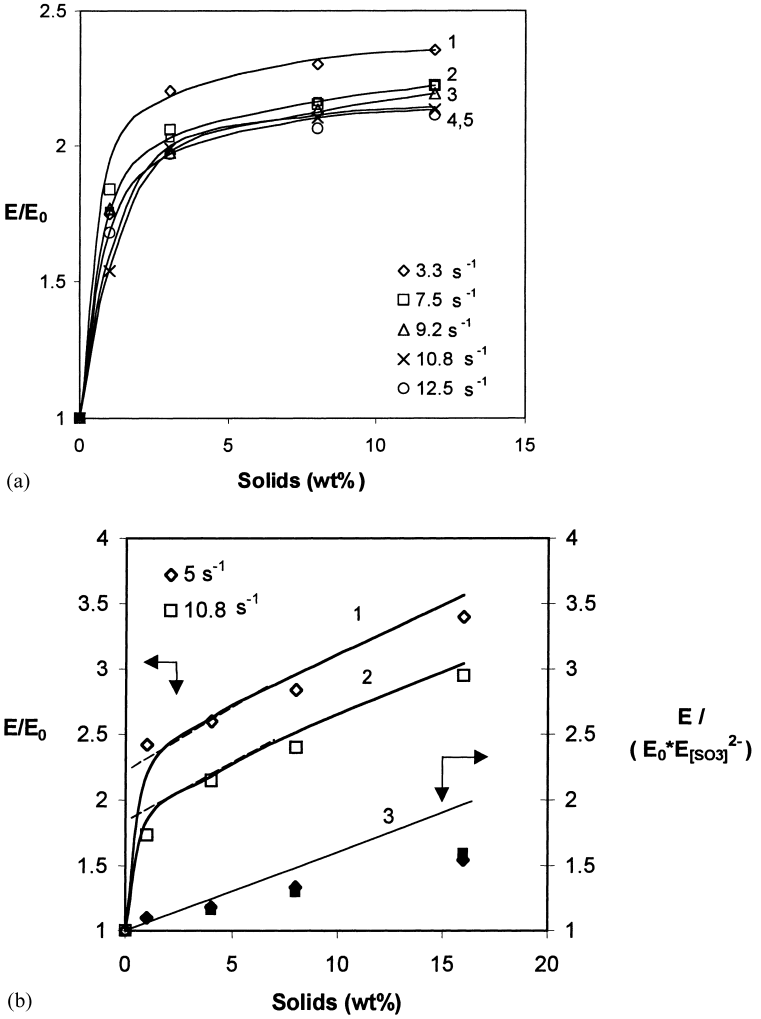

Fig. 4. Enhancement factor ratio as a function of solid concentration. (Initial pressure $= 0.8 \times 10^5$ Pa, $T = 298$ K). (a) SO_2 absorption in $Ca(OH)_2$ slurry (Lines 1, 2, 3, 4 and 5: from theoretical values of enhancement factor predicted according to Uchida et al. [2]). (b) SO_2 absorption in $Mg(OH)_2$ slurry (◆:experimental values of $(E/(E_0^*(E/E_0)_{w=0}))$ at $10.8\,s^{-1}$, ■: experimental values of $(E/(E_0^*(E/E_0)_{w=0}))$ at $5\,s^{-1}$, Line 1 and 2: theoretical values with correct N/w values, Line 3: theoretical values predicted by Model II [8,10]).

$[SO_3]^{2-}$ is produced in the film by the reaction of SO_2 and the hydroxide ions (reaction I) and also by the reaction of $[HSO_3]^-$ and the hydroxide ions (reaction II). The consumption of $[SO_3]^{2-}$, however, occurs only by its reaction with SO_2. Hence the rate of generation of $[SO_3]^{2-}$ is greater than its consumption in the film, due to which the concentration of $[SO_3]^{2-}$ starts building up in the film. The concentration of $[SO_3]^{2-}$ in the film is larger than its concentration in the bulk liquid due to which $[SO_3]^{2-}$ diffuses into the liquid bulk.

The enhancement caused by the reaction between SO_2 and the $[SO_3]^{2-}$ formed was assessed by extrapolating the observed enhancement in the presence of solids to that for a saturated solution of magnesium hydroxide, that is $(E/E_0)_{w=0}$.

Table 6
Experimental values of the enhancement factor for $SO_2/Ca(OH)_2$ slurry system

Solids (wt.%)	Enhancement factor (E)					E/E_0				
	$3.3\,s^{-1}$	$7.5\,s^{-1}$	$9.2\,s^{-1}$	$10.8\,s^{-1}$	$12.5\,s^{-1}$	$3.3\,s^{-1}$	$7.5\,s^{-1}$	$9.2\,s^{-1}$	$10.8\,s^{-1}$	$12.5\,s^{-1}$
0	1.11	1.04	1.02	1.02	1.02	1	1	1	1	1
1	2.13	1.83	1.57	1.86	1.71	1.93	1.77	1.54	1.84	1.68
4	2.35	2.13	2.02	1.90	2.02	2.13	2.05	1.97	1.87	1.96
8	2.56	2.14	2.12	2.13	2.19	2.31	2.06	2.07	2.1	2.15
16	2.58	2.14	2.18	2.22	2.26	2.34	2.06	2.13	2.19	2.22

Table 7
Values of the solid dissolution parameter at different solid loading for $SO_2/Mg(OH)_2$ slurry system

Speed (s^{-1})	Solids (kg/m^3)	$k_L \times 10^5$ (m/s)	$z = D/k_L$ (μm)	N/w
5	0.01	4.4	31.8	11.31
	0.04	4.4	31.8	11.31
	0.08	4.4	31.8	11.31
	0.16	4.4	31.8	11.31
10.8	0.01	5.6	25.0	7.58
	0.04	5.1	27.5	9.14
	0.08	4.9	28.6	9.91
	0.16	4.9	28.6	9.91

This value was found experimentally to be 1.8 at $10.8\,s^{-1}$ and 2.4 at $5\,s^{-1}$ (Fig. 4b).

To estimate the contribution of solids in the observed enhancement factor, the degree of enhancement which was also caused due to the reaction II was avoided by Sada et al. [9] by converting the ratio E/E_0 to the quantity $(E/E_0 - (E/E_0)_{w=0} - 1))$, where the quantity $((E/E_0)_{w=0} - 1)$ corresponded for the extra enhancement due to the reaction II. Model II predicts the data of the effect of addition of solids on the enhancement factor at different values of N/w. Sada et al. [9] thus, estimated the value of N/w to be 12.3 by comparing their experimental findings with the theoretical values predicted by Model II. However, their procedure of calculating the contribution of solids to the enhancement factor does not seem to be correct as enhancement factors are factorial, i.e. are multiplicative and hence they should not be subtracted. So it is more logical to define the total enhancement factor E as $E = E_0 \times E_s \times E_{[SO_3]^{2-}}$.

Hence, in our calculations, the ratio of E/E_0 was converted to the quantity $(E/(E_0 \cdot (E/E_0)_{w=0}))$, to estimate the effect of suspended solids alone on the enhancement factor where the quantity $(E/E_0)_{w=0}$ counts for the additional increase in the enhancement due to reaction II which is represented by $E_{[SO_3]^{2-}}$. The values of $(E/(E_0(E/E_0)_{w=0}))$ are represented as the dark points in Fig. 4b and are also indicated in Tables 8 and 9. These dark points show the contribution to the enhancement in the rate of absorption due to the presence of the suspended solids only. For comparison, the values predicted by Model II for $N/w = 12.3$ is shown in the form of a solid line (3) in Fig. 4b. The difference in the values between our experimental findings and the line 3, especially at higher solid loading, is due to the more accurate procedure for the estimation of solid dissolution parameter and the multiplicative approach to estimate the contribution of solids in the enhancement. With the correct values of N (as estimated by us), Sada et al.'s theoretical values won't match with their experimental findings. But because they followed a theoretical approach, they estimated a higher value of N and hence could compare their theoretical data with the experimental.

For the slurry process, the Sherwood number can be defined as $Sh = k_s d_p / D_B$ which gives the value of $N = Sh(6w/\rho)(z_L/d_p)^2$.This indicates that the quantity N/w is dependent on Sh and d_p. For calculation of N/w, $Sh = 2$ was assumed in our calculations which resulted into the value of $N/w = 11.31$ for $5\,s^{-1}$. The values of N/w for the different solid loading are shown in Table 7. These values of N/w were used to calculate the theoretical enhancement factors due to the presence of solids using Eq. (22), which are indicated by the two solid curves (1 and 2) represented in Fig. 4b.

Table 8
Experimental values of enhancement factor for $SO_2/Mg(OH)_2$ slurry system

Solids (wt.%)	Enhancement factor (E)		E/E_0	
	$5\,s^{-1}$	$10.8\,s^{-1}$	$5\,s^{-1}$	$10.8\,s^{-1}$
0	1.02	1.03	1	1
1	2.46	1.78	2.42	1.73
4	2.65	2.21	2.61	2.15
8	2.89	2.46	2.84	2.40
16	3.36	3.03	3.30	2.95

Table 9
Experimental values of the enhancement caused due to the solid particles alone for $SO_2/Mg(OH)_2$ slurry system

Solids (wt.%)	$(E/(E_0{}^*(E_{[SO_3]^{2-}})))$	
	$5\,s^{-1}$	$10.8\,s^{-1}$
0	1	1
1	1.1	1
4	1.18	1.16
8	1.29	1.29
16	1.54	1.59

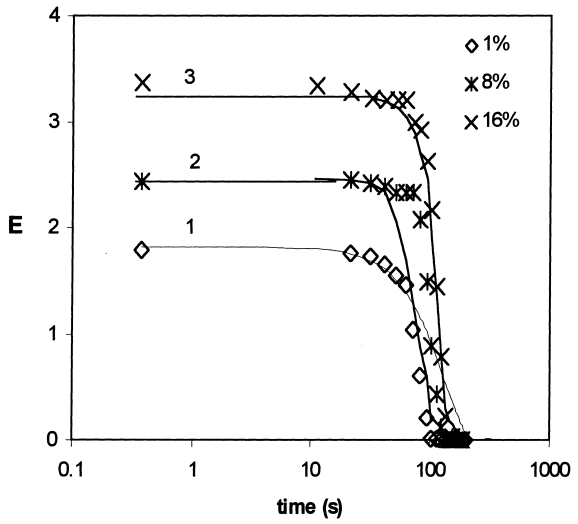

Fig. 5. Variation of enhancement of SO_2 absorption with time. (System: $SO_2/Mg(OH)_2$ slurry, speed = $5\,s^{-1}$, initial pressure = 0.8×10^5 Pa, $T = 298$ K, Line 1, 2, 3: theoretical values predicted according to Sada et al. [9]).

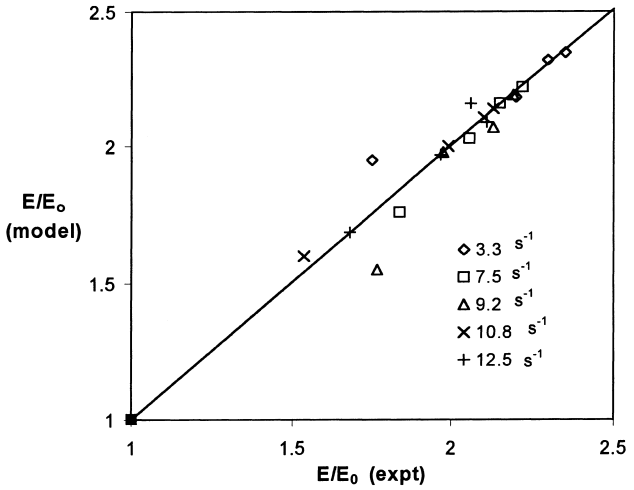

Fig. 6. Parity plot showing the comparison of experimental and theoretical values (according to the model of Uchida et al. [2]) of the enhancement factor ratio for SO_2–$Ca(OH)_2$ slurry system. (Initial pressure $= 0.8 \times 10^5$ Pa, $T = 298$ K, Solids = 0–12 wt.%).

6.3. Effect of batch time

Fig. 5 shows the variation of the enhancement factor with time as observed for reactive SO_2 absorption in a $Mg(OH)_2$ slurry. It can be seen that the enhancement is constant at the start for some time and then decreases and ultimately becomes zero. Initially, at higher partial pressures of SO_2, the consumption of $[SO_3]^{2-}$ by reaction II is balanced by its regeneration by reaction III. Hence the enhancement remains constant. Then, as the absorption of SO_2 proceeds, the pressure in the reactor and also the amount of the gas absorbed reduces and hence results in a reduction of the enhancement. The solid lines are the theoretical values. For the calculation of the variation of the theoretical enhancement factor with time, the variation of theoretical pressure with time was calculated initially, by substituting Eq. (22) in Eq. (6) and integrating it. The variation of the enhancement factor with time was then recalculated from Eq. (6) by putting theoretical values of pressure.

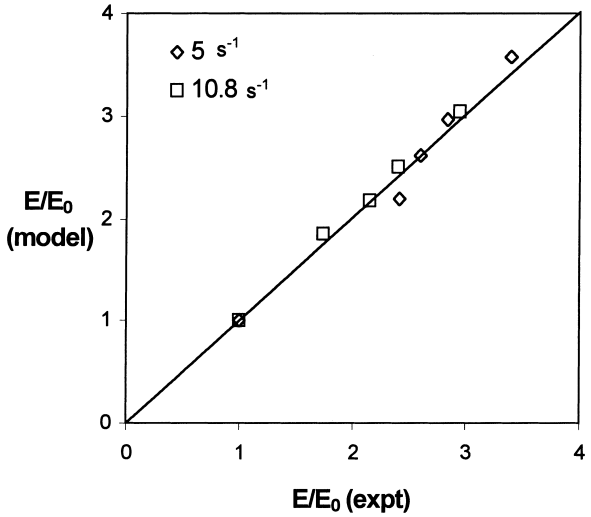

Fig. 7. Parity plot showing the comparison of experimental and theoretical values (according to Sada et al. [9]) of the enhancement factor ratio for the SO_2–$Mg(OH)_2$ slurry system. (Initial pressure $= 0.8 \times 10^5$ Pa, $T = 298$ K, Solids = 0–12 wt.%).

6.4. Comparison of experimental and theoretical

Figs. 6 and 7 show the comparison between experimental and theoretical values of the enhancement factor owing to the presence of solid particles for both calcium and magnesium hydroxide in the slurries, respectively. It is evident that the experimental and the model values are in good agreement.

7. Conclusions

The absorption of sulfur dioxide into aqueous slurries containing fine suspended reactive particles of calcium and magnesium hydroxide was performed in a stirred cell at relatively high mass transfer coefficients. The enhancement of the mass transfer due to the presence of fine particles increased with the solid concentration. Experimental data on the absorption rates were compared with the theoretical predictions using two different models i.e. a model proposed by Uchida et al. [2] for the $Ca(OH)_2$ slurry and the two reaction plane model proposed by Sada et al. [9] for the $Mg(OH)_2$ slurry. For the later system the results could be accurately described by a new approach defining an overall enhancement factor E which is built up as $E = E_0 \times E_s \times E_{[SO_3]^{2-}}$ with E_s and $E_{[SO_3]^{2-}}$ being the factorial enhancement factors due to the effects of suspended solids and the reaction of SO_2 and $[SO_3]^{2-}$, respectively. The enhancement factor thus calculated proved to predict the values observed experimentally very well.

References

[1] C.A. Ramachandran, M.M. Sharma, Absorption with fast reaction in a slurry containing sparingly soluble fine particles, Chem. Eng. Sci. 24 (1969) 1681.

[2] S. Uchida, K. Koide, M. Shindo, Gas absorption with fast reaction into a slurry containing fine particles, Chem. Eng. Sci. 30 (1975) 644.

[3] E. Sada, H. Kumazawa, M.A. Butt, Single gas absorption with reaction in a slurry containing fine particles, Chem. Eng. Sci. 32 (1977) 1165.

[4] E. Sada, H. Kumazawa, Y. Sawada, I. Hashizume, Absorption of sulfur dioxide into aqueous slurries of sparingly soluble fine particles, Chem. Eng. Sci. 35 (1980) 771.

[5] E. Sada, H. Kumazawa, T. Hoshino, Absorption of lean SO_2 in aqueous solutions of Na_2CO_3 and desorption of CO_2, Chem. Eng. J. 18 (1979) 125.

[6] E. Sada, H. Kumazawa, M.A. Butt, Absorption of sulfur dioxide in aqueous slurries of sparingly soluble fine particles, Chem. Eng. J. 19 (1977) 131.
[7] E. Sada, H. Kumazawa, M.A. Butt, Simultaneous absorption with reaction in a slurry containing fine particles, Chem. Eng. Sci. 32 (1977) 1499.
[8] E. Sada, H. Kumazawa, M.A. Butt, Single and simultaneous absorptions of lean SO_2 and NO_2 into aqueous slurries of $Ca(OH)_2$ or $Mg(OH)_2$ particles, Chem. Eng. Sci. 12 (2) (1979) 111.
[9] E. Sada, H. Kumazawa, Y. Sawada, I. Hashizume, Kinetics of absorption of lean sulfur dioxide into aqueous slurries of calcium carbonate and magnesium hydroxide, Chem. Eng. Sci. 36 (1981) 149.
[10] E. Sada, H. Kumazawa, M.A. Butt, T. Sumi, Removal of dilute SO_2 by aqueous slurries of $Mg(OH)_2$ particles, Chem. Eng. Sci. 32 (1977) 972.
[11] V.D. Mehta, M.M. Sharma, Mass transfer in mechanically agitated gas–liquid contactors, Chem. Eng. Sci. 26 (1971) 461.
[12] A.A.C.M. Beenackers, W.P.M. van Swaaij, Mass transfer in gas–liquid slurry reactors, Chem. Eng. Sci. 48 (18) (1993) 3109.
[13] H. Yagi, K. Okamoto, K. Naka, H. Hikita, Chemical absorption of CO_2 and SO_2 into $Ca(OH)_2$ slurry, Chem. Eng. Sci. 26 (1984) 1.
[14] E. Sada, H. Kumazawa, M.A. Butt, Absorption of SO_2 in aqueous slurries of sparingly soluble fine particles, Chem. Eng. Sci. 19 (1980) 131.
[15] E. Sada, H. Kumazawa, I. Hashizume, Further consideration on chemical absorption mechanism by aqueous slurries of sparingly soluble fine particles, Chem. Eng. Sci. 36 (1981) 639.
[16] E. Sada, H. Kumazawa, N. Nishimu, Absorption of SO_2 into aqueous double slurries contatining limestine and $Mg(OH)_2$, AIChE J. 29 (1) (1983) 60.
[17] C. Laohavichitra, K. Muroyama, S.H. Weng, L.S. Fan, Absorption of SO_2 by calcium hydroxide solution in a wetted wall column: Effect of magnesium hydroxide, magnesium carbonate and magnesium sulfite additives, Chem. Eng. Sci. 37 (10) (1982) 1982.
[18] E. Sada, H. Kumazawa, C.H. Lee, Chemical absorption into conc. slurry: absorption of CO_2 and SO_2 into aq. conc. slurries of $Ca(OH)_2$, Chem. Eng. Sci. 39 (1984) 117.
[19] E. Sada, H. Kumazawa, H. Nishimu, Absorption of SO_2 into aqueous double slurries containing limestone and $Mg(OH)_2$, Chem. Eng. Sci. 29 (1983) 60.
[20] W.P. Bronikowska, K.J. Rudzinski, Absorption of SO_2 in aqueous systems, Chem. Eng. Sci. 46 (9) (1991) 2281.